

Pauli-principle driven correlations in four-neutron nuclear decays

P.G. Sharov,^{1,*} L.V. Grigorenko,^{1,2,3} A.N. Ismailova,¹ and M.V. Zhukov⁴

¹*Flerov Laboratory of Nuclear Reactions, JINR, 141980 Dubna, Russia*

²*National Research Nuclear University “MEPhI”, 115409 Moscow, Russia*

³*National Research Centre “Kurchatov Institute”, Kurchatov sq. 1, 123182 Moscow, Russia*

⁴*Department of Physics, Chalmers University of Technology, 41296 Göteborg, Sweden*

Mechanism of simultaneous non-sequential four-neutron ($4n$) emission (or “true” $4n$ -decay) has been considered in five-body approach. It is demonstrated that $4n$ -decay fragments should have specific energy and angular correlations reflecting strong spacial correlations of “valence” neutrons orbiting in their $4n$ -precursors. Due to the Pauli exclusion principle, the valent neutrons are pushed to the symmetry-allowed configurations in the $4n$ -precursor structure, which causes a “Pauli focusing” effect. Prospects of observation of the Pauli focusing have been considered for the $4n$ precursors ^7H and ^{28}O . Fingerprints of their nuclear structure or/and decay dynamics are predicted.

Introduction. — In the last decade there was a great progress in the studies of three-body decays (e.g. two-proton radioactivity) [1]. In contrast to “conventional” two-body decays, three-body decays encrypt a lot of additional information in the momentum (energy and angular) correlations of the decay products. Theoretical studies indicate that both effects of the initial nuclear structure and the decay mechanism may show up in the core+ $n+n$ and core+ $p+p$ fragment correlation patterns in various ways [2–12].

With development of experimental techniques, more and more “complicated” nuclear systems become available for studies. One of such complicated cases are isotonic neighbors of the $4n$ halo systems located beyond the neutron drip-line, which decay via $4n$ -emission. The examples of such systems which are now actively studied by experiment are ^7H and ^{28}O . The $4n$ -emission phenomenon is expected to be widespread beyond the neutron drip-line, and other possible candidates for such a decay mode, e.g. ^{18}Be can be mentioned. Their ground states are expected to be unbound with $E_T \lesssim 2$ MeV (E_T is energy above the $4n$ decay threshold), and the decay mechanism can be assumed as “true” $4n$ emission: there are no sequential neutron emission, i. e. all neutrons are emitted simultaneously. For low decay energies with $E_T \lesssim 300$, keV such a decay mechanism may lead to very long lifetimes characterized in terms of $4n$ radioactivity [13]. From experimental side only $4p$ emission from ^8C has been studied so far [14]. However, this decay has sequential $^8\text{C} \rightarrow 2p + (^6\text{Be} \rightarrow 2p + \alpha)$ mechanism.

In the case of $4n$ -emission (core+ $4n$ decay) the five-body correlations encrypt enormously more information compared to the three-body case: the complete correlation pattern is described by 11-dimensional space compared to the 2-dimensional one. The decay amplitude antisymmetrization should decrease the effective dimension of the correlation space, but there should be still a lot. The question can be asked here “What are physically meaningful signals in this wealth of information?”

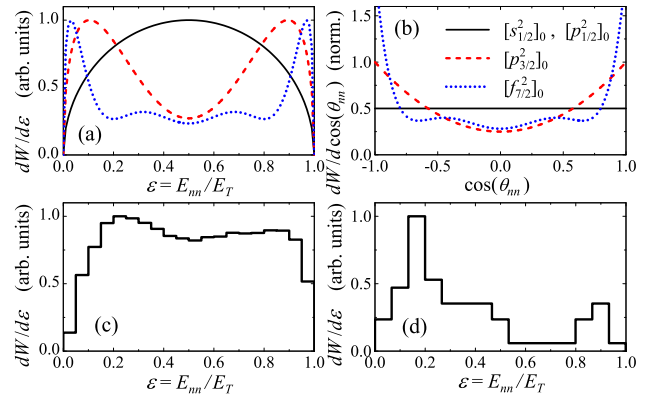


FIG. 1. (color online) Pauli focusing for three-body decays with valence $2n$ in configurations $[s_{1/2}]_0$, $[p_{1/2}]_0$, $[p_{3/2}]_0$, and $[f_{7/2}]_0$. Panel (a) shows n - n energy distribution, panel (b) shows n - n angular distribution obtained neglecting n - n final state interaction. Panels (c) and (d) show the energy p - p distributions observed for ^6Be [8] and ^{45}Fe [6].

This work demonstrates that core- n and n - n energy and angular distributions may provide important information on the dominant configurations involved in the $4n$ decay. Moreover, the studies of correlated $\{i-j, k-l\}$ patterns of energy and angular distributions may give unique signatures for orbital configurations involved in the decay (numbers $i \neq j$, $k \neq l$ enumerate different selections of decay products).

The concept of “Pauli focusing” was proposed in [15] and further discussed e.g. in [16, 17] for the bound state structure of three-body core+ $n+n$ systems. It was demonstrated that due to the Pauli exclusion principle, population of orbital configurations $[l_{j_1} \otimes l_{j_2}]_J$ for the valence nucleons may induce strong spatial correlations depending on the specific values of j_1 , j_2 , and J . Various forms of such correlations were actively discussed as integral part of the two-nucleon halo phenomenon and now them are well experimentally confirm.

For bound states the theoretically predicted Pauli focusing correlations are “hidden” in the nuclear interior and can be accessed experimentally only by indirect way.

* sharovpavel@jinr.ru

In contrast, in the three-body decay process these internal correlations may directly exhibit themselves in the momentum distributions of the decay products. This is illustrated in Fig. 1 for the three-body decays of the $[l_j^2]_J$ orbital configurations (direct decay into continuum is assumed). The $[s_{1/2}]_0$ and $[p_{1/2}]_0$ configurations produce phase-space function $\sqrt{\varepsilon(1-\varepsilon)}$ in the nucleon-nucleon channel and isotropical angular distribution between nucleons, while the $[p_{3/2}]_0$ and $[f_{7/2}]_0$ configurations give strong $2N$ correlations. This issue is also illustrated in Fig. 1 (c,d) by the experimentally observed energy distributions of fragments in the $2p$ decays of ${}^6\text{Be}$ and ${}^{45}\text{Fe}$ [1, 6, 8, 18]. Qualitatively, the signature of the Pauli focusing, the double-hump structure characteristic for $[p_{3/2}]_0$ configuration, can be easily seen in both cases. However, for quantitative explanation two more effects require consideration: (i) nucleon-nucleon final state interaction (FSI) and (ii) subbarrier tunneling to configurations with lower angular momenta (and hence easier penetration), see Refs. [1, 7, 9, 19]. In the process of penetration through the subbarrier region, the following changes in the orbital populations take place

$${}^6\text{Be} : \quad [p_{3/2}]_0 \rightarrow C_{23}[p_{3/2}]_0 + C_{01}[s_{1/2}]_0, \quad (1)$$

$${}^{45}\text{Fe} : \quad [f_{7/2}]_0 \rightarrow C_{67}[f_{7/2}]_0 + C_{23}[p_{3/2}]_0. \quad (2)$$

The complete three-body model studies give $C_{23} \approx C_{01}$ in ${}^6\text{Be}$ and $C_{67} \ll C_{23}$ in ${}^{45}\text{Fe}$, which explains the difference in qualitative and quantitative descriptions of experimental spectra.

The Pauli focusing for 5-body systems was discussed in [20] by example of ${}^8\text{He}$ nucleus described by the $\alpha+4n$ model. Complicated spatial correlation patterns were predicted. The same case was considered in details in [21]. In analogy with three-body case we may expect that Pauli focusing correlations found in the bound five-body system should exhibit themselves in decays if such a systems are located above the five-body breakup threshold. However, the questions *whether* and *how* such correlations can be used to extract physical information have never been addressed so far.

Phase-space distributions. — Before we discuss a physically meaningful signal, connected with nuclear structure and decay dynamics, we should first understand the “kinematically defined” correlations, which are connected with phase-space of several particles. The phase-space V_4 for 5 particles can be defined by 4 energies $E_i = \varepsilon_i E_T$ corresponding to 4 Jacobi vectors in the momentum space

$$dV_4 \sim \delta(E_T - \sum_i \varepsilon_i E_T) \sqrt{\varepsilon_1 \varepsilon_2 \varepsilon_3 \varepsilon_4} d\varepsilon_1 d\varepsilon_2 d\varepsilon_3 d\varepsilon_4. \quad (3)$$

The phase-space energy distribution between any two fragments $dV_1/d\varepsilon_1$ and correlated phase-space distribution of two energies $dV_{12}/d\varepsilon_1 d\varepsilon_2$ can be obtained by the respective integrations of Eq. (3)

$$dV_1 \sim \sqrt{(1-\varepsilon_1)^7 \varepsilon_1} d\varepsilon_1, \quad (4)$$

$$dV_{12} \sim (1-\varepsilon_1 - \varepsilon_2)^2 \sqrt{\varepsilon_1 \varepsilon_2} d\varepsilon_1 d\varepsilon_2. \quad (5)$$

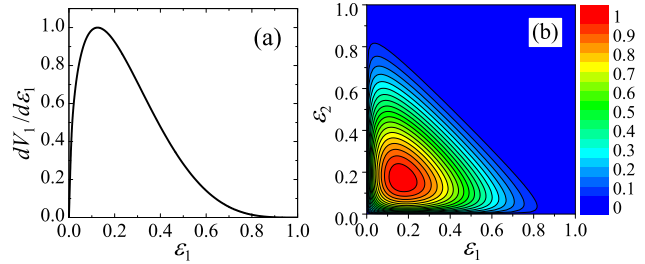


FIG. 2. (color online) Five-body phase-space (a) one- and (b) two-dimensional energy distributions of Eqs. (4) and (5).

The distributions (4) and (5) are shown in Fig. 2(a) and (b). The distribution (4) has a maximum at $\varepsilon_1 = 1/8$ and a mean energy value $\varepsilon_1 = 1/4$, the distribution (5) has a maximum at $\varepsilon_1 = \varepsilon_2 = 1/6$.

In addition to the distributions of Eqs. (4) and (5), the correlated two-dimensional $\{i-k, n-m\}$ ($i \neq k, n \neq m$) energy and angular distributions may be constructed. For core+4n decays in total five topologically nonequivalent such two-dimensional distributions exist, see Fig. 3 (the others can be reduced to them by permutations of indistinguishable particles). It is evident that “topologically disconnected” distributions $cn-nn$ and $nn-nn$ of Fig. 3 (cols. 3,5) are equivalent to distributions of Eq. (5) and Fig. 2 (b) as Jacobi variables are “disconnected” in the same sense. It can be seen that the other correlated distributions have quite distinctive shapes even in the phase-space case.

Model for dynamics of 5-body decay. — The differential decay probability is defined as

$$dW \sim |T|^2 dV_4 \prod_{i=1..4} d\Omega_i.$$

In this work we consider very simple model for core+ $n_1+n_2+n_3+n_4$ decay with analytical Ansatz for the decay amplitude

$$T = \mathcal{A} [\prod_{i=1..4} A_{cn_i}(l_i, j_i, \mathbf{p}_{cn_i})]_J, \quad (6)$$

where $A_{cn_i}(l_i, j_i, \mathbf{p}_{cn_i})$ is single particle decay amplitude and \mathbf{p}_{cn_i} , l_i and j_i are momentum, angular momentum, and total spin conjugated to radius-vector \mathbf{r}_{cn_i} between core and nucleon number i . The amplitude T has define total spin J and is antisymmetrized (operator \mathcal{A} above) for permutation of four valence nucleons. The Monte-Carlo procedure is used to compute various momentum distributions. The single-particle amplitudes are approximated by R-matrix type expression

$$A_{cn_i}(l_i j_i, \mathbf{p}_{cn_i}) = \frac{1}{2} \frac{a_{l_i j_i} \sqrt{\Gamma_{cn_i}(E_{cn_i})}}{E_{r,cn_i} - E_{cn_i} - i\Gamma_{cn_i}(E_{cn_i})/2}, \quad (7)$$

where E_{r,cn_i} is resonance energy in the cn_i channel, while $\Gamma_{cn_i}(E_{cn_i})$ is its standard R-matrix width as a function of energy. This reasonable approximation becomes very precise in the limit of infinite core mass.

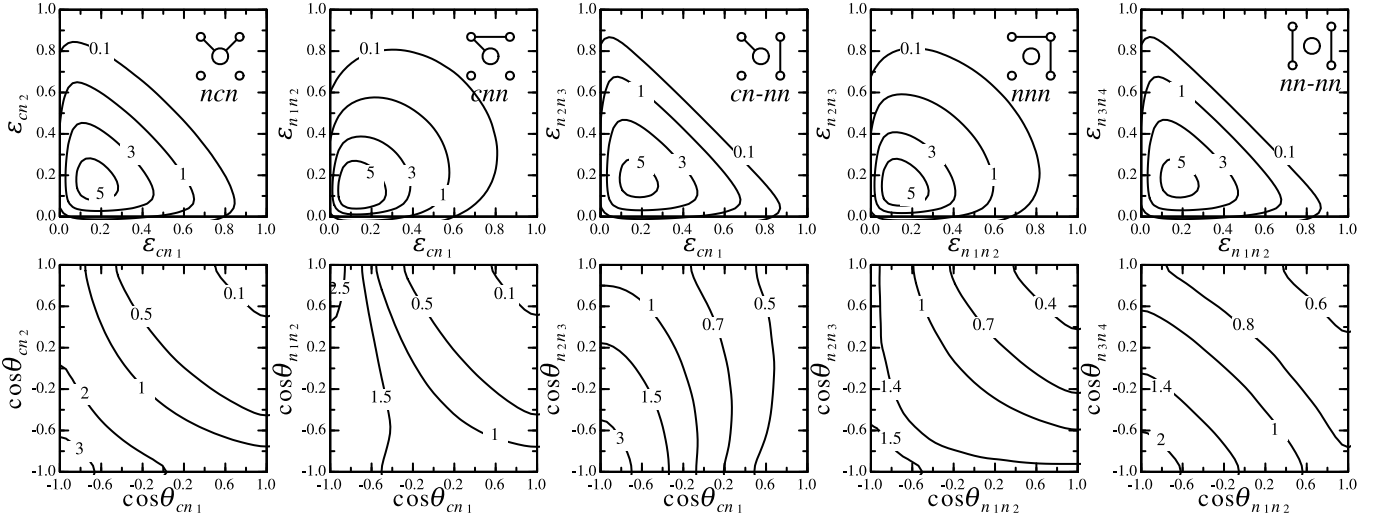


FIG. 3. Nonequivalent five-body phase-space correlated energy (upper row) and angular (lower row) distributions for core+4n decays. The sketches in the upper row panels illustrate the selection of the correlated pairs of fragments: *ncn*, *cnn*, *cn-nn*, *nnn*, *nn-nn*. For presentation purpose, the angular distributions are normalized to value of 4 (the isotropic distribution then has constant value of unity).

In order to estimate the possible effect of *n-n* FSI, the Eq. (6) can be modified as

$$T = \mathcal{A} \left[\prod_{i=1..4} A_{cn_i}(\mathbf{p}_{cn_i}) \prod_{i>k} A_{n_i n_k}(\mathbf{p}_{n_i n_k}) \right]. \quad (8)$$

The amplitude $A_{n_i n_k}$ is the (typical for the Migdal-Watson-type approximations) zero-range expression for an *s*-wave *n-n* scattering

$$A_{n_i n_k} = \frac{a_s}{1 - i p_{n_i n_k} a_s}, \quad (9)$$

where $a_s = -18.9$ fm is the singlet scattering length in the *n-n* channel. This approximation provides no control of actual total spin in the particular n_i - n_k channel. Thus the effect of *n-n* FSI should be much overestimated here as, *on average*, only two pairs of neutrons (out of six possible selections) can be both in relative spin $S = 0$ state and in relative *s*-wave simultaneously. So, we may consider Eq. (8) as an upper-limit estimate of the effect.

Scenarios of 5-body decay. — The five-body decays are so far not studied. Thus, in our discussion we follow the assumed qualitative analogy of 3-body and 5-body decay dynamics. Let us consider the examples of ^7H and ^{28}O whose internal structure is expected to be dominated by $[p_{3/2}]_0$ and $[d_{3/2}]_0$ configurations, respectively. In the process of decay these configurations may drift to configurations with lower angular momenta in analogy with Eqs. (1) and (2)

$$^7\text{H}: [p_{3/2}]_0 \rightarrow C_{2323}[p_{3/2}]_0 + C_{0123}[s_{1/2}^2 p_{3/2}]_0, \quad (10)$$

$$^{28}\text{O}: [d_{3/2}]_0 \rightarrow C_{4343}[d_{3/2}]_0 + C_{0143}[s_{1/2}^2 d_{3/2}]_0 + C_{0123}[s_{1/2}^2 p_{3/2}]_0. \quad (11)$$

The one-dimensional energy and angular distributions for the pure above-mentioned configurations in the core-*n*

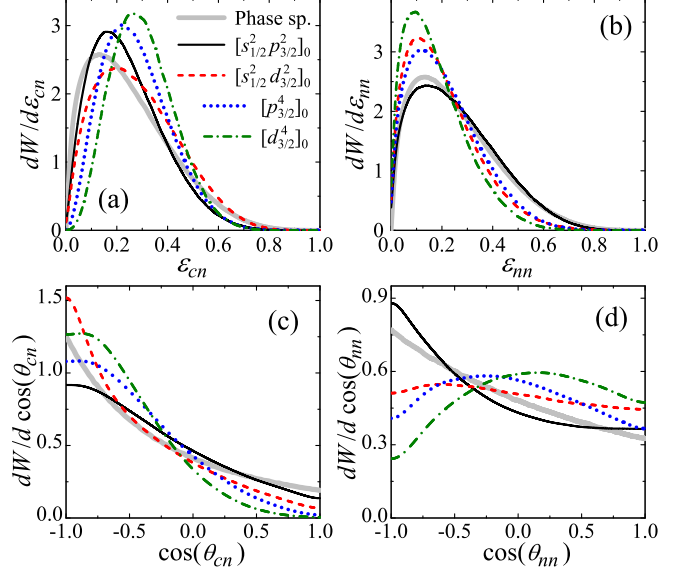


FIG. 4. (color online) Normalized energy (a,b) and angular (c,d) distributions in the core-*n* (a,c) and *n-n* (b,d) channels of 4*n*-decay for all different pure 4*n* configurations which can be found in Eqs. (10) and (11). The decay energy $E_T = 500$ keV. The reference phase-space distributions are shown by the thick gray lines.

and *n-n* channels are shown in Fig. 4. On average, the increase of angular momentum “content” of the component leads to the increase of the mean energy in the core-*n* and the corresponding decrease in the *n-n* channels. The respective angular distributions have quite distinctive patterns. So, one may see a strong effect of definite orbital configuration already in these observables.

The Pauli focusing effect on two-dimensional corre-

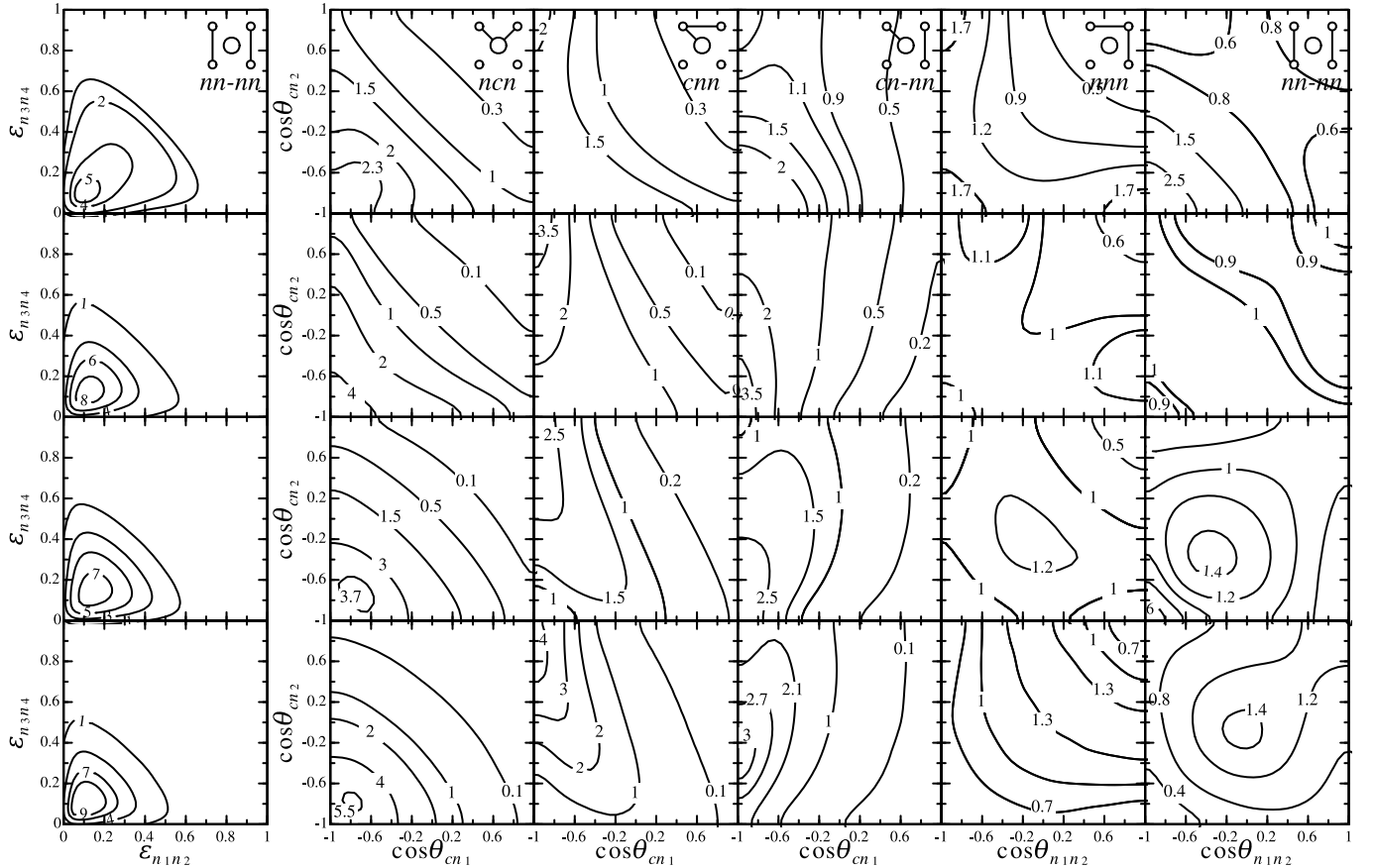


FIG. 5. Correlated energy distributions for nn - nn topology (col. 1) and correlated angular distributions for ncn (col. 2), cnn (col. 3), cn - nn (col. 4), nnn (col. 5), and nn - nn (col. 6) topologies. Configurations from Eqs. (10) and (11) correspond to the pure components $[s_{1/2}^2 p_{3/2}]_0$ (row 1), $[s_{1/2}^2 d_{3/2}]_0$ (row 2), $[p_{3/2}]_0$ (row 3), and $[d_{3/2}]_0$ (row 4). The decay energy $E_T = 500$ keV.

lated energy distributions is illustrated in Fig. 5 (col. 1) for one selected nn - nn topology. All four considered cases are quite distinguishable from the phase-space distributions, as well as from each other. Among them the case of $[s_{1/2}^2 p_{3/2}]_0$ configuration has a specially strong qualitative distinction. Even stronger variability can be seen in the correlated angular distributions, which are systematically surveyed in Fig. 5 (cols. 2–6). The correlation patterns show great variability: all of them are strongly different from the phase-space distributions and from each other. Therefore the full set of predicted correlation patterns provide clear signatures on dominating $4n$ -decay configurations: some pairs of plots for two different configurations may look similar, however, selection other pair should provide distinctive signal. This feature may be used in planning of future experiments and the data analysis.

Discussion. — The experience of three-body decay studies tell us that the effect of configuration mixing in the final state may have strong effect on the observed correlations. However, the simplified predicted correlations may be relevant in two limiting cases. (i) For decay energies above the typical barrier energies (e.g. $E_T > 2 - 4$ MeV) the effect of configuration mixing may be small,

and then one-configuration approximation may be precise enough. However, n - n FSI should have growing effect on the distributions in such a limiting case. (ii) For deep subbarrier energies $E_T < 100 - 300$ keV, the decay should proceed via the $[s^2 p^2]_0$ configurations which have the lowest possible barriers. For the case (ii) our predictions should be very precise with improving precision in the limit $E_T \rightarrow 0$.

Effect of n - n FSI is known to strongly influence the three-body energy and angular correlations. In three-body case this effect is expected to vanish as decay energy goes below $E_T \sim 100$ keV, see, e.g. [12]. Distributions of Fig. 6 obtained by Eq. (8) for $[s_{1/2}^2 p_{3/2}]$ configuration illustrate how important can be the effect of n - n FSI in five-body decay. We can see in Fig. 6 (b) that the effect is reasonably small under $E_T < 300$ keV and can be neglected under $E_T < 100$ keV. Curious to note that the modifications of the n - n energy distribution by the n - n FSI for $E_T \lesssim 2$ MeV is near perfectly described by the Migdal-Watson type expression

$$\frac{dW}{d\varepsilon_{nn}} = \frac{dW_{ps}}{d\varepsilon_{nn}} \frac{a_s^2(\text{eff})}{1 + 2M_{nn} E_T \varepsilon_{nn} a_s^2(\text{eff})}, \quad (12)$$

where $dW_{ps}/d\varepsilon_{nn}$ is the phase-space distribution and

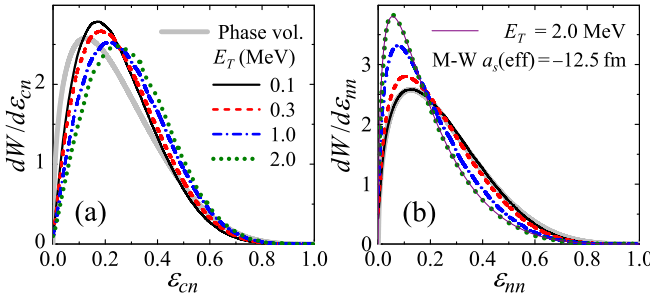


FIG. 6. (color online) Effect of n - n FSI on energy distributions in core- n (a) and n - n (b) channels at different decay energies E_T for $[s_{1/2}p_{3/2}]$ configuration. Solid, dashed, dash-dotted, and dotted lines correspond to E_T of 0.1, 0.3, 1.0, and 2.0 MeV, respectively. Phase-space is shown by thick grey line.

$a_s(\text{eff}) = -12.5$ fm is a sort of effective scattering length, see thin solid curve in Fig. 6 (b) practically coincide with $E_T = 2$ MeV results. Thus we can qualitatively state here that the “effective intensity” of the n - n FSI within

the emitted in the decay of such configuration “tetraneutron” is around 44% of the “vacuum intensity” evaluated as a_s^2 (with $a_s = -18.9$ fm).

Conclusion. — In this work we have for the first time theoretically studied the correlations in emission of four nucleons in the nuclear 5-body decay. We have demonstrated that for true five-body decays of core+4 n systems the *Pauli focusing* — the cumulative effects of antisymmetrization and population of definite orbital configurations — may lead to distinctive correlation patterns. We propose to study the full set of the two-dimensional correlated energy or/and angular distributions for derivation of information concerning the quantum-mechanical 4 n -decay configuration. In total five distinct correlated distributions are available for analysis and they seem to form a unique “fingerprint” of the decay quantum state. Reconstruction of all these distributions require complete kinematical characterization of the core+4 n decay, which is presumably within the reach of modern experiment.

Acknowledgments. — This work for PGS and LVG was supported in part by the Russian Science Foundation grant No. 17-12-01367. The authors are grateful to Dr. I. Mukha for helpful discussions.

[1] M. Pfützner, M. Karny, L. V. Grigorenko, and K. Riisager, Rev. Mod. Phys. **84**, 567 (2012).
[2] L. V. Grigorenko and M. V. Zhukov, Phys. Rev. C **68**, 054005 (2003).
[3] I. Mukha, E. Roeckl, L. Batist, A. Blazhev, J. Döring, H. Grawe, L. Grigorenko, M. Huyse, Z. Janas, R. Kirchner, M. L. Commara, C. Mazzocchi, S. L. Tabor, and P. V. Duppen, Nature **439**, 298 (2006).
[4] L. V. Grigorenko and M. V. Zhukov, Phys. Rev. C **76**, 014008 (2007).
[5] I. Mukha, L. Grigorenko, K. Sümmerer, L. Acosta, M. A. G. Alvarez, E. Casarejos, A. Chatillon, D. Cortina-Gil, J. M. Espino, A. Fomichev, J. E. García-Ramos, H. Geissel, J. Gómez-Camacho, J. Hofmann, O. Kiselev, A. Korsheninnikov, N. Kurz, Y. Litvinov, I. Martel, C. Nociforo, W. Ott, M. Pfützner, C. Rodríguez-Tajes, E. Roeckl, M. Stanoiu, H. Weick, and P. J. Woods, Phys. Rev. C **77**, 061303 (2008).
[6] L. V. Grigorenko, T. D. Wiser, K. Miernik, R. J. Charity, M. Pfützner, A. Banu, C. R. Bingham, M. Cwiok, I. G. Darby, W. Dominik, J. M. Elson, T. Ginter, R. Grzywacz, Z. Janas, M. Karny, A. Korgul, S. N. Liddick, K. Mercurio, M. Rajabali, K. Rykaczewski, R. Shane, L. G. Sobotka, A. Stoltz, L. Trache, R. E. Tribble, A. H. Wuosmaa, and M. V. Zhukov, Phys. Lett. B **677**, 30 (2009).
[7] L. V. Grigorenko, T. D. Wiser, K. Mercurio, R. J. Charity, R. Shane, L. G. Sobotka, J. M. Elson, A. H. Wuosmaa, A. Banu, M. McCleskey, L. Trache, R. E. Tribble, and M. V. Zhukov, Phys. Rev. C **80**, 034602 (2009).
[8] I. A. Egorova, R. J. Charity, L. V. Grigorenko, Z. Chajecki, D. Coupland, J. M. Elson, T. K. Ghosh, M. E. Howard, H. Iwasaki, M. Kilburn, J. Lee, W. G. Lynch, J. Manfredi, S. T. Marley, A. Sanetullaev, R. Shane, D. V. Shetty, L. G. Sobotka, M. B. Tsang, J. Winkelbauer, A. H. Wuosmaa, M. Youngs, and M. V. Zhukov, Phys. Rev. Lett. **109**, 202502 (2012).
[9] L. V. Grigorenko, I. G. Mukha, and M. V. Zhukov, Phys. Rev. Lett. **111**, 042501 (2013).
[10] K. W. Brown, R. J. Charity, L. G. Sobotka, Z. Chajecki, L. V. Grigorenko, I. A. Egorova, Y. L. Parfenova, M. V. Zhukov, S. Bedoor, W. W. Buhro, J. M. Elson, W. G. Lynch, J. Manfredi, D. G. McNeel, W. Reviol, R. Shane, R. H. Showalter, M. B. Tsang, J. R. Winkelbauer, and A. H. Wuosmaa, Phys. Rev. Lett. **113**, 232501 (2014).
[11] K. W. Brown, R. J. Charity, L. G. Sobotka, L. V. Grigorenko, T. A. Golubkova, S. Bedoor, W. W. Buhro, Z. Chajecki, J. M. Elson, W. G. Lynch, J. Manfredi, D. G. McNeel, W. Reviol, R. Shane, R. H. Showalter, M. B. Tsang, J. R. Winkelbauer, and A. H. Wuosmaa, Phys. Rev. C **92**, 034329 (2015).
[12] L. V. Grigorenko, J. S. Vaagen, and M. V. Zhukov, Phys. Rev. C **97**, 034605 (2018).
[13] L. V. Grigorenko, I. G. Mukha, C. Scheidenberger, and M. V. Zhukov, Phys. Rev. C **84**, 021303(R) (2011).
[14] R. J. Charity, J. M. Elson, J. Manfredi, R. Shane, L. G. Sobotka, B. A. Brown, Z. Chajecki, D. Coupland, H. Iwasaki, M. Kilburn, J. Lee, W. G. Lynch, A. Sanetullaev, M. B. Tsang, J. Winkelbauer, M. Youngs, S. T. Marley, D. V. Shetty, A. H. Wuosmaa, T. K. Ghosh, and M. E. Howard, Phys. Rev. C **84**, 014320 (2011).
[15] B. Danilin, M. Zhukov, A. Korsheninnikov, V. Efros, and L. Chulkov, Sov. J. Nucl. Phys. **48**, 766 (1988), [Yad. Fiz. **48**, 1208 (1988)].
[16] M. Zhukov, B. Danilin, D. Fedorov, J. Bang, I. Thompson, and J. Vaagen, Phys. Rep. **231**, 151 (1993).
[17] P. Mei and P. V. Isacker, Annals of Physics **327**, 1162 (2012).

- [18] L. V. Grigorenko, K. Langanke, N. B. Shul'gina, and M. V. Zhukov, Phys. Lett. B **641**, 254 (2006).
- [19] K. Miernik, W. Dominik, Z. Janas, M. Pfützner, L. Grigorenko, C. R. Bingham, H. Czyrkowski, M. Cwiok, I. G. Darby, R. Dabrowski, T. Ginter, R. Grzywacz, M. Karny, A. Korgul, W. Kusmierz, S. N. Lid-
- dick, M. Rajabali, K. Rykaczewski, and A. Stolz, Phys. Rev. Lett. **99**, 192501 (2007).
- [20] M. V. Zhukov, A. A. Korsheninnikov, and M. H. Smedberg, Phys. Rev. C **50**, R1 (1994).
- [21] P. Mei and P. V. Isacker, Annals of Physics **327**, 1182 (2012).